JOURNAL OF Applied Polymer SCIENCE

Epoxy modification with poly(vinyl acetate) and poly(vinyl butyral). I. Structure, thermal, and mechanical characteristics

T. V. Brantseva,[1] V. I. Solodilov,[2] S. V. Antonov,[1] I. Y. Gorbunova,[3] R. A. Korohin,[2] A. V. Shapagin,[4] N. M. Smirnova[1]

[1]Polymer Composites and Adhesives Laboratory, A.V. Topchiev Institute of Petrochemical Synthesis, Russian Academy of Sciences, 29 Leninsky Prospect, Moscow 119991, Russia

[2]Laboratory of Reinforced Plastics, N.N. Semenov Institute of Chemical Physics, Russian Academy of Sciences, 4 Kosygin Street, Moscow 119991, Russia

[3]Department of Polymer Processing Technology, Mendeleev University of Chemical Technology of Russia, Miusskaya Square 9, Moscow 125047, Russia

[4]Laboratory of Structural and Morphological Investigations, A.N. Frumkin Institute of Physical Chemistry and Electrochemistry, Russian Academy of Sciences, 31/4 Leninsky Prospect, Moscow 119071, Russia

Correspondence to: T.V. Brantseva (E-mail: brantseva@ips.ac.ru or t_brantseva@mail.ru)

ABSTRACT: Efficiency of the application of high strength heat resistant thermoplastics for improving fracture toughness and impact properties of epoxy resins motivated authors to try large-scale production thermoplastics for the same purpose. Epoxy/anhydride systems were modified by up to 8 wt % poly(vinyl acetate) (PVAc) and up to 6 wt % poly(vinyl butyral) (PVB). In epoxy–PVAc blends it was possible to obtain morphologies with continuous thermoplastic phase. However, only sea-island morphologies with a very small size of PVB-rich phase were observed in epoxy–PVB matrices. The former type of morphology allowed a notable 2.4-fold increase in the fracture toughness of epoxy resin and simultaneous up to 30% decrease in its' impact strength. The latter type of morphology caused a notably lower (45%) enhancement of the epoxy fracture toughness combined with a 50% increase in its' impact strength. © 2016 Wiley Periodicals, Inc. J. Appl. Polym. Sci. **2016**, *133*, 44081.

KEYWORDS: blends; mechanical properties; phase behavior; thermoplastics; thermosets

Received 29 March 2016; accepted 15 June 2016
DOI: 10.1002/app.44081

INTRODUCTION

Epoxy resins are one of the most widely produced thermosetting resins, with such an extensive popularity explained by their ease in processing, high mechanical and adhesion characteristics, good electric insulating properties, chemical resistance and relatively low shrinkage during curing.[1] However, multiple microcracks initiation and growth takes place during the epoxy products exploitation, which results in the premature product failure. By now, epoxy toughness enhancement was achieved by introduction of rubber modifiers,[2,3] active diluents[4] or thermoplastic polymers.[5–13] Active diluents are substances, allowing decrease in the epoxy system viscosity and participating in the curing reaction, for example, diglycidyl ether of diethylene glycol. Unfortunately, usage of both rubber modifiers and active diluents led to a decrease in the heat resistance of epoxy matrices. Moreover, usage of rubber modifiers led to a notable decrease in the Young's modulus and tensile strength and dramatical increase in viscosity.[2,3] High strength heat resistant thermoplastics, used for epoxy resin toughening, can substantially enhance fracture strength and impact properties of the epoxy resins[5–13] whilst not compromising their heat resistance or tensile strength and modulus.

In most cases phase-separated structures are obtained, when epoxy systems are modified by either rubbers or thermoplastics. It should be noted, however, that there is no definite viewpoint on the optimal structure of the cured epoxy–thermoplastic matrices, although most authors suggest that phase separation is one of the main conditions required for the enhanced mechanical[5,6,8,9] and heat resistant properties.[9,14,15]

It is well known that epoxy–thermoplastic blends are mostly used in high-tech industry, when the heat resistance of the matrix should be high enough. Consequently, expensive high strength heat resistant thermoplastics are used in this case, such as polysulfone,[5–7] phenoxy resin,[8] polyethersulfone,[9,10] poly(arylene ether ketone),[11] and polyetherimide (PEI).[12,13] However, there are some cases, when high heat resistance of the system is

not required. In these cases, cheap large-scale production thermoplastics that would not contribute to higher price of the modified matrix could also be tried. Poly(vinyl acetate) (PVAc) and poly(vinyl butyral) (PVB) could be considered for this purpose. Several works describing their behavior in the blends with epoxy resins have been published by now.[16–19] For instance, Prolongo *et al.*,[17,18] and Zheng *et al.*[16] studied curing kinetics, thermal and some of the mechanical properties of the epoxy–PVAc blends. They confirmed phase inversion in these systems that started at 10–15 wt % PVAc, but were able to obtain only a moderate increase in Young's modulus and fracture toughness—up to ~20–30%, in case of 20 wt % PVAc in the epoxy matrix. At the same time, in Ref. 6 up to fourfold increase in the fracture toughness of epoxy matrix was reported in case of polysulfone incorporation. Moreover, Prolongo *et al.*[18] also observed a notable (~40%) tensile strength decrease at 20 wt % PVAc content. To summarize publications on epoxy–PVAc blends, for PVAc modifier no impact strength studies were carried out, although the corresponding properties could definitely be improved.

In Refs. 19 and 20 epoxy–PVB blends cured by the phenolic curing agents—intended for use as coating films—were studied. An increase in the adhesion properties was reported, but only when substantial quantities of PVB were used—up to 50 wt % of thermoplastic modifier. The fracture toughness and impact properties of PVB–epoxy systems are not described in the existing publications. Moreover, the content of the PVB in them is too high, it might be reasonable to explore lower contents.

So, based on all mentioned earlier, the objective of our research was to study the effect of PVAc and PVB modifiers incorporation on the thermal and mechanical properties (including impact characteristics) of the system. Investigation of modifiers content influence on the glass transition temperature, storage and loss moduli, fracture toughness and impact strength was to be done for this purpose as well as studying the morphology of the cured systems. Taking into account possibility of PVB interaction with the anhydride hardener as it was shown in ref. 21, using the modifiers chosen could result in obtaining matrices with different phase state.

Another point worth considering was the curing agent influence. In almost all cases of epoxy resins modification amine curing agents were used. Anhydride cured systems are not usually considered in such cases, Refs. 22 and 23 being rare exceptions. Even in these works only phase separation and curing kinetics were studied, and mechanical properties were not investigated at all. However, application of anhydride hardeners could result in obtaining systems with high climate and heat resistance (which could be quite important, if we use thermoplastics with low T_g that could give a trend to lowering T_g of the whole system).[24] Moreover, such notable changes in the system composition—transition from amine to anhydride hardener—could lead to the changes in the phase state of the systems studied since modifier solubility in epoxy system, and kinetics of phase transition processes, could differ in these cases.[25] So, usage of the anhydride cured system was considered to be of interest in this case.

EXPERIMENTAL

Materials

Hot curing epoxy system Araldite® LY 556/Aradur® 917/Accelerator DY 070 provided by Huntsman (USA) was selected for our work. Here Araldite® LY 556 is an epoxy resin based on diglycidyl ether of bisphenol-A (DGEBA), Aradur® 917 is an anhydride hardener and Accelerator DY 070 is an imidazole accelerator. The following resin/hardener/accelerator ratio was used: 100/90/0.5 (w/w/w). Chemical formulae of the main substances are shown in Figure 1.

PVAc of the M100 grade was provided by Vitakhim (Russia). Its molecular weight (2.1×10^5 Da) was determined by measurement of intrinsic viscosity of PVAc solutions in tetrahydrofurane at 25 °C by Ostwald viscometer. The following values of Mark–Houwink constants were used for molecular weight calculations: $K = 1.6 \times 10^{-4}$ dL/g, $a = 0.7$.[26]

PVB of the KA grade was provided by Volna–Polymer (Russia). Its molecular weight (3.2×10^4 Da) was also determined by measurement of intrinsic viscosity of solutions in tetrahydrofurane at 25 °C by Ostwald viscometer The following values of Mark–Houwink constants were used: $K = 2.9 \times 10^{-4}$ dL/g, $a = 0.72$.[27]

Blends Preparation and Curing

The compositions of epoxy system with the PVAc were prepared using the following procedure:

1. The resin was degassed in a vacuum oven at 100–120 °C for 1 h.
2. The required amount of the thermoplastic was added.
3. The blend was mixed by the overhead stirrer until complete modifier dissolution.
4. The blend was degassed in a vacuum oven at 100–120 °C for 0.5 h.
5. The hardener was added to the blend.
6. The accelerator was added to the blend.
7. The composition was mixed for 5 min at 80 °C for homogenization.

Then the composition was poured into a special silicon mold and curing was carried out in the following regime: 90 °C 3 h + 120 °C 12 h.

PVAc content was 2, 4, and 8 wt % (calculated in relation to the resin + hardener weight), PVB content was 2, 4, and 6 wt %. In case of PVB another sequence was used: step 1 → step 5 → step 7→ step 2→ step 3→ step 4→ step 6→ step 7. The reasons for such changes are specified below, in "Solubility Tests" section.

Materials Characterization

DSC Measurements. A TA Instruments (USA) DSC 2920 calorimeter was used to measure the glass transition temperatures of the cured samples. DSC thermograms were obtained using a constant heating rate of 20 °C/min, scanning was carried out from 0 to 200 °C in argon atmosphere. Samples of 10–15 mg were used. To assure reproducible thermograms free from thermal history effects, two cycles of heating were used for DSC measurements. Glass transition temperatures were calculated from the second cycles of the DSC thermograms.

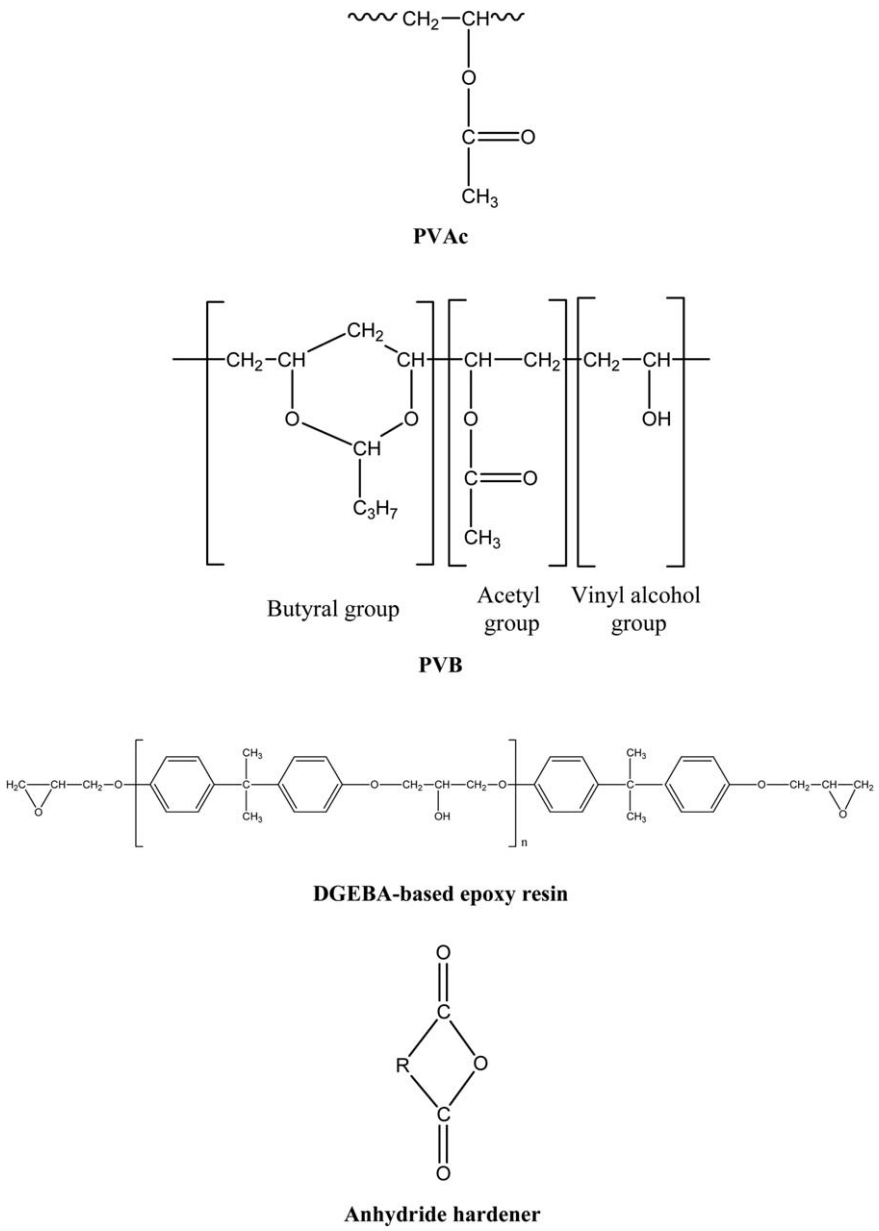

Figure 1. Chemical structures of the main substances.

Torsion Pendulum Measurements. Cured samples were tested at the torsion pendulum MK-3 (Khimavtomatika, Russia), with free torsion oscillations. Its measurement principle is based on the transformation of damping mechanical oscillations into electric signal by means of a special photoelectric receiver. Logarithmic damping ratio ζ and oscillations period T were measured and the loss tangent tan δ was calculated using the following formula:

$$\tan\ \delta = \frac{\zeta}{\pi}\left(\frac{1}{1+\zeta^2/4\pi^2 - T_s^2/T_0}\right) \quad (1)$$

where ζ is a logarithmic damping ratio, T_s is an oscillation period for the system with the sample, T_0 is the same value in the absence of a sample.

Shape factor F and shear modulus G' were calculated as follows:

$$F = \frac{bd^3}{3l}\left(1 - 0.63\frac{d}{b}\right) \quad (2)$$

$$G' = \frac{I}{F}\left(\frac{4\pi^2+\zeta^2}{T_s^2} - \frac{4\pi^2}{T_0^2}\right) \quad (3)$$

where b is the sample's width, d is the sample's thickness, and l is a sample's length.

Glass transition temperatures of the samples were determined as a maximum of the loss tangent versus temperature curve. Samples of approximately 64 mm length, 7 mm width, and 1.4 mm thickness were tested.

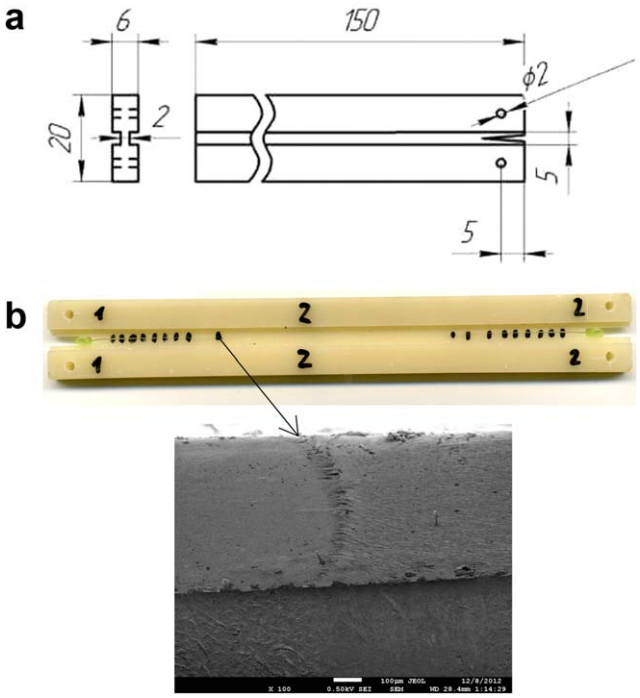

Figure 2. Scheme of the sample used for the fracture toughness measurements (a) and one the samples tested (b); the black lines show the areas of the crack propagation. Callout shows the picture of the crack front propagation taken by the electron microscope. [Color figure can be viewed in the online issue, which is available at wileyonlinelibrary.com.]

DMA Measurements. DMA was performed in a three-point bending mode using a Netzsch Artemis DMA 242E device. Cured samples of the following dimensions were taken: 40 mm × 8 mm × 5 mm. Measurements were done at 1 Hz frequency, in the 30–250 °C temperature range at a heating rate of 1 °C/min. The maxima on the tan δ–temperature curves were determined, indicating α-relaxation processes associated with the glass transition of the systems studied. Storage modulus changes in the course of the temperature increase were also considered.

Fracture Toughness Measurements. The technique used for the fracture toughness measurements was developed earlier on the basis of ref. 28.

After curing the samples were allowed to cool at room temperature and then shaped at the lathe and grinding machine to obtain their final design (Figure 2). The thickness of the groove used for directing the crack did not exceed 2 mm. The initial notch for crack initiation of 0.1 mm thickness was made by the razor. The notch was situated at 8–10 mm distance from the through-holes for the sample fixation in the testing machine grips.

Tensile testing was carried out at Instron-1122 testing machine. The sample was fixed in the Instron grips using the through-holes shown in Figure 2 and the tensile testing was carried out with a cross-head speed of 1 mm/min at room temperature (20–22 °C). The force was increasing up to a certain critical value, when the crack started to propagate. After the crack propagation stopped, the sample was unloaded, and the loading cycles were repeated till the final cracking of the sample. Scheme of the typical loading diagram in this case is shown in Figure 3.

Both halves of the sample were taken out of the appliance and the length of the crack developed at each stage of the loading was measured, together with the distance from the through-holes for the sample fixation to the point where propagation of the crack started. This point is clearly seen by the band perpendicular to the direction of the crack propagation [Figure 2(b)].

Fracture toughness for each stage of the crack propagation was calculated as:

$$G_{IC}=2\gamma=\frac{P_i\delta_i k}{2l_i w_i}, \tag{4}$$

where γ is a specific surface energy of the crack propagation, P_i—maximum force achieved when the propagation of the ith crack starts, δ_i—compliance (deviation of the sample tabs at the point of the force application) for the ith crack, l_i—distance from the centers of the through-holes for the sample fixation to the end of the ith crack, w_i—an average surface width during the ith crack propagation; k—constant of the sample, depending on its' stiffness (in our case $k = 3$ ref. 28).

The first and the last cycles were excluded from the calculations as it was recommended in ref. 28. The results were obtained as an average value from at least 14 cycles for each sample, and 3 samples were tested for each system.

Determination of the Impact Properties. Impact testing was performed in a three-point bending mode using a special device based on the spring impact machine, described in detail in ref. 7. Unnotched samples of 32 mm × 5 mm × 5 mm size were taken for measurements. Low-velocity impact loading was carried out with the 4 m/s loading rate (impact energy 13.0 J) allowing measurement of impact strength σ_i and failure energy E_i, calculated according to the formulas:

$$\sigma_i=\frac{3P_{max}l}{2bh^2} \tag{5}$$

$$E_i=v\int_{t_0}^{t_i}P(t)dt \tag{6}$$

where v is the impactor velocity when it contacts the sample, l, b, and h are the sample's length, width and height

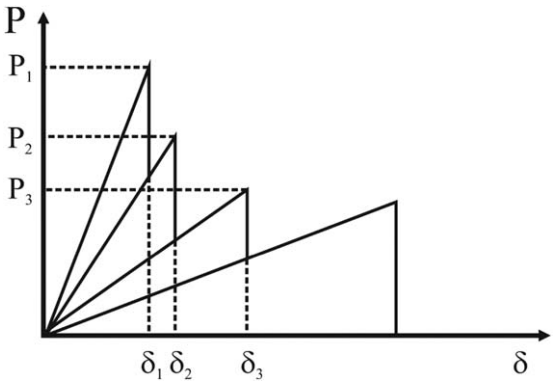

Figure 3. Schematic relationship between the force P and deviation of the sample tabs δ.

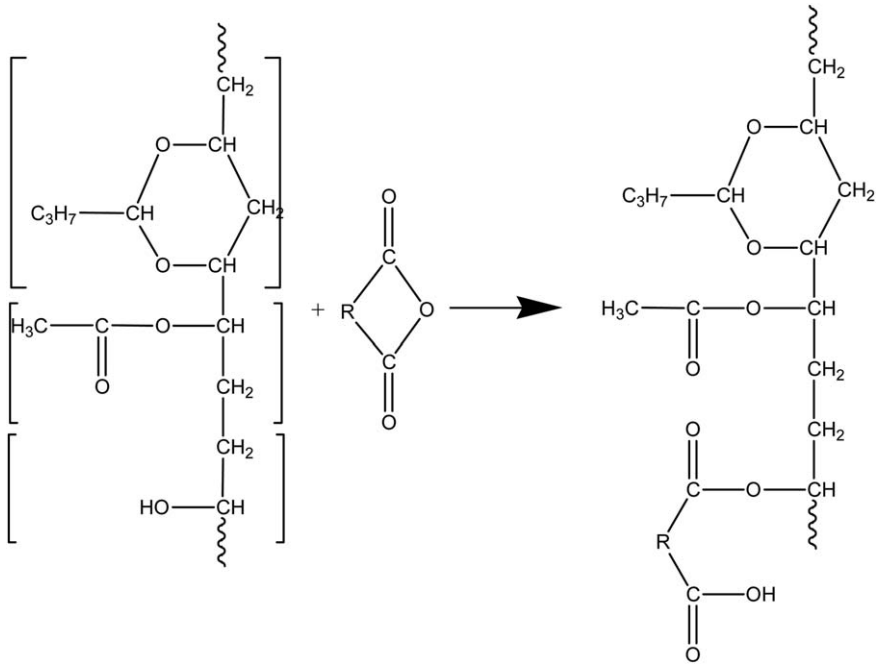

Figure 4. Scheme of the possible interaction between PVB and anhydride hardener.

correspondingly, and the integral part is the area under the force–time loading curve taken from the beginning t_0 till a certain moment t_i. Since we were calculating the total failure energy, area under the whole curve was used.

Microscopy. The structure and morphology of cured systems were studied with scanning electron microscopy (SEM) and transmission electron microscopy (TEM). SEM was performed on JSM U-3 (Jeol, Japan), equipped with the XRD Eumex microanalyzer, and TEM was performed on TEM-301 (Philips, The Netherlands).

The investigated surfaces of cured samples were obtained by fracturing in liquid nitrogen. To reveal the phase structure, high-frequency oxygen plasma etching was applied. For this purpose, we used the E306A (Edwards Coating System, USA) vacuum chamber and the technique described in ref. 29. The discharge source was a high frequency self-generating short-wave generator with 100 W capacity. Oxygen pressure in the chamber was 2×10^{-1} mmHg, and the discharge frequency was 10 MHz. Etching was carried out for at least 40 min.

Preparation of the SEM samples was carried out using a standard technique[30] with the carbon coating by thermal vacuum spraying. For TEM morphologies investigations replica technique was used.[31]

RESULTS

Solubility Tests

As a first stage of our work, solubility of PVAc and PVB in the chosen epoxy system at room temperature was checked visually. According to the literature,[16–20] we expected to obtain true solutions of the thermoplastics in the epoxy system. However, the problems with miscibility could still arise, since quite a significant quantity of liquid curing agent was used. In case of PVAc, curing agent addition did not change its solubility in epoxy oligomer. Quite a different situation occurred when PVB was used. Solubility of PVB in epoxy resin in absence of the hardener was very low, well below 1 wt %. On the other hand, PVB readily dissolved in the mixture of epoxy resin with anhydride hardener. The possible explanation of this fact might be an interaction of PVB hydroxyl groups with the curing agent as it was already mentioned.[32] The scheme of the possible interaction is demonstrated in Figure 4.

So, due to the primarily solubility data obtained, we changed the procedure of the epoxy–thermoplastic blends preparation for PVB as described earlier. It should also be noted, that the highest content of PVB easily solved in epoxy resin + hardener mixture was 6 wt %, which was used as a maximum content for epoxy–PVB systems.

Mechanical Properties of the Blends

As it was mentioned in the "Introduction" section, incorporation of heat resistance thermoplastics such as polysulfones and polyetherimides[5–8] sometimes improved the fracture toughness and/or impact properties of epoxies quite significantly. However, sometimes an increase was not so great, and also, high quantities of thermoplastics were required to obtain noticeable effects: 15 − 20 wt %. In our case, only up to 6 − 8 wt % modifier contents were used, so we did not expect notable fracture toughness enhancements.

The pictures of the samples tested are demonstrated in Figure 5. It is clearly seen from the Figure 5, that samples with PVAc turned opaque after curing, which should be indicative of the phase separation processes. Samples with PVB are still transparent, which could be possible if: (a) no phase separation is observed; (b) microphase separation takes place and the size of

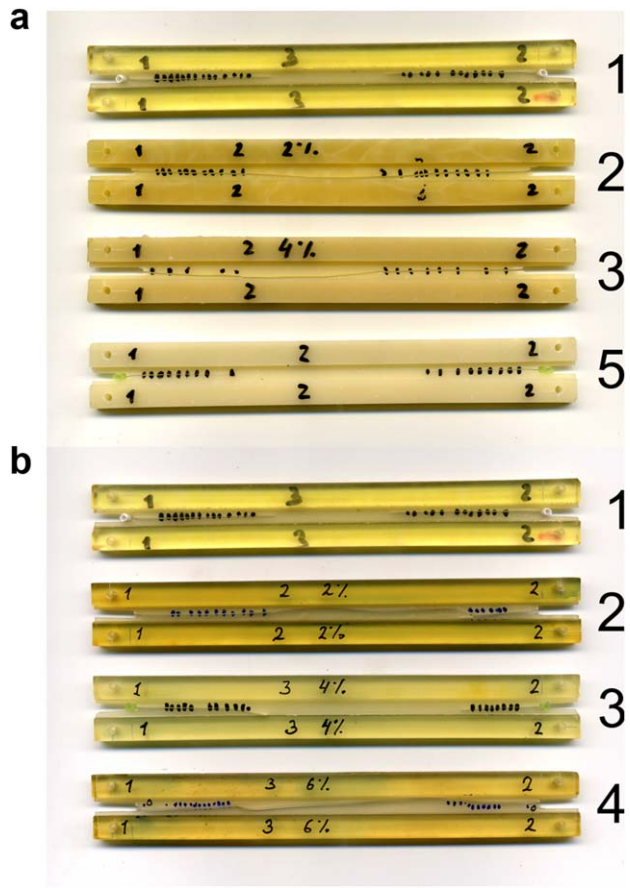

Figure 5. Epoxy–thermoplastic samples after fracture toughness testing. Thermoplastic modifier: (a) PVAc, (b) PVB. Modifier content: (1) 0 wt %, (2) 2 wt %, (3) 4 wt %, (4) 6 wt %, and (5) 8 wt %. [Color figure can be viewed in the online issue, which is available at wileyonlinelibrary.com.]

the inclusions of forming phase is comparable with optical wavelength.

The resulting values of the fracture toughness are presented in Figure 6. It can be seen that incorporation of both thermoplastics resulted in an increase in the fracture toughness of the epoxy matrix. In case of PVB a dependency with a maximum at 4 wt % modifier was obtained, and corresponding increase in G_I was 45%. Further addition of PVB results in a fracture toughness decrease. It should also be noted that the data scattering is quite small, which confirms reliability of the results obtained.

Behavior of epoxy–PVAc systems was different, fracture toughness constantly grows with PVAc content, although this growth slows down after incorporation of 4 wt % PVAc. An increase in this case is much higher—up to 2.4-fold if compared with initial epoxy resin values. However, quite a high data scattering was obtained in case of 4 wt % PVAc in epoxy matrix, which could be indicative of some intermediate structure formed at this content. It could be supposed that various patterns of G_I concentration dependences and the magnitude of G_I increase are connected with differences in the phase state of the systems and correspondingly, in the mechanisms responsible for the fracture toughness changes.

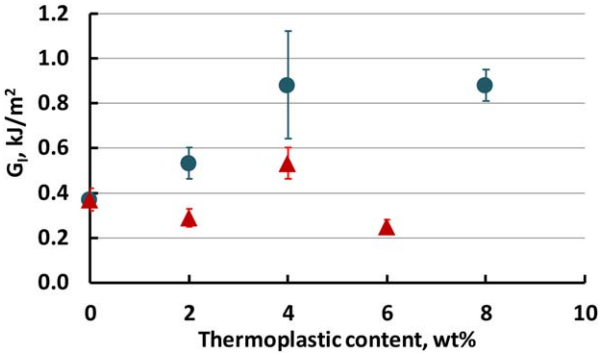

Figure 6. Fracture toughness of epoxy–thermoplastic matrices. Thermoplastics: (●) PVAc, (▲) PVB. [Color figure can be viewed in the online issue, which is available at wileyonlinelibrary.com.]

The next stage of the investigation was to check the influence of the modifiers on the low-velocity impact properties. Low-velocity impact loading diagrams obtained for our systems are presented in Figure 7. Incorporation of the modifier does not change the shape of the diagrams. In all the cases, a quick samples failure is observed after the maximum load was reached. However, thermoplastics incorporation changes the maximum force value at the diagrams. For PVAc notable decrease in the

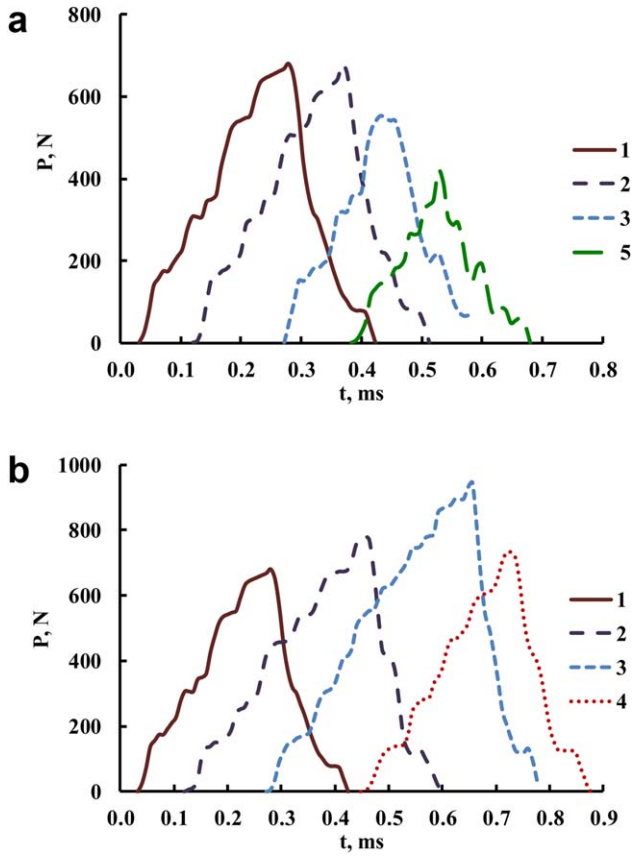

Figure 7. Loading diagrams of epoxy–PVAc (a) and epoxy–PVB (b) systems obtained at low-velocity impact loading. Thermoplastic content: (1) 0 wt %, (2) 2 wt %, (3) 4 wt %, (4) 6 wt %, and (5) 8 wt %. [Color figure can be viewed in the online issue, which is available at wileyonlinelibrary.com.]

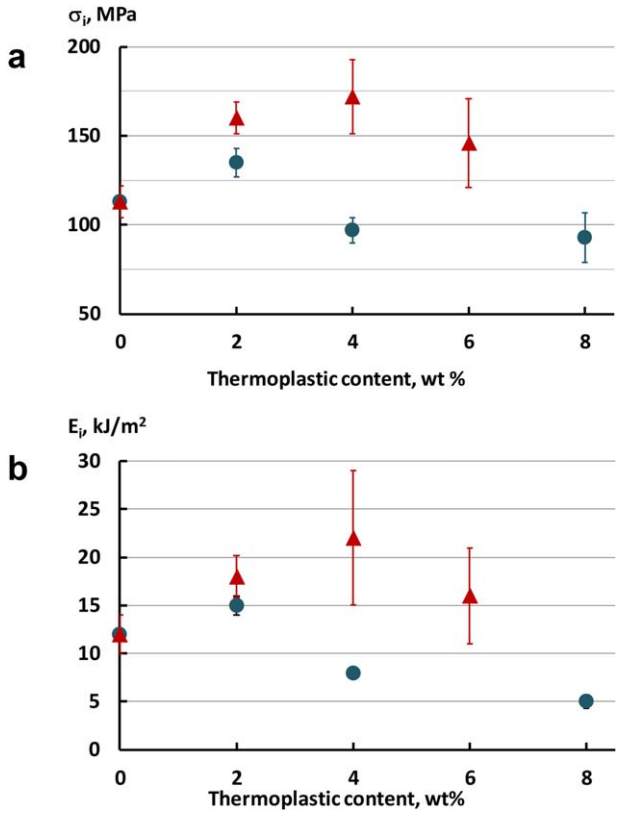

Figure 8. Impact strength (a) and failure energy (b) of epoxy–thermoplastic matrices. Thermoplastic modifier: ● PVAc, ▲ PVB. [Color figure can be viewed in the online issue, which is available at wileyonlinelibrary.com.]

maximum force is observed, starting from 4 wt % modifier. For epoxy–PVB systems a substantially increased maximum force was observed at 4 wt % thermoplastic, with all the other values being on the level of unmodified system or slightly higher. In both cases the maximum force was observed at 4 wt % modifier. The time required for the material to failure also changes and varies from 0.15 to 0.4 ms. Similar diagrams with the same trends were obtained earlier for epoxy–polysulfone systems, with the time to failure varying from 0.15 to 0.3 ms.[33]

Loading diagrams were used to calculate impact strength σ_i and failure energy E_i values for the systems studied, and the resultant curves are demonstrated in Figure 8. According to the data obtained, for PVAc the maximum impact characteristics are observed at 2 wt %, with a small 20–25% increase in σ_i and E_i in comparison with pristine epoxy matrix. Further PVAc incorporation leads to a 20–60% decrease in the measured values depending on the PVAc content. PVB incorporation shifts the maximum to 4 wt %. For PVB the overall increase in σ_i and E_i is more prominent, up to 52% and 83% correspondingly. Differences in the modifiers influence on the epoxy resin impact characteristics can be caused by the different failure mechanisms in our systems (Figure 9). In some cases, crack branching took place, with the sample fragments formed after the impact. This failure mechanism was observed for the pristine epoxy, epoxy–PVB, and epoxy–2 wt % PVAc matrices. These are all the cases when impact properties enhancement was noticed. Alternatively, when the crack propagated across the specimen without any branching, the sample was destroyed almost instantly. In such cases a decrease in the failure energy was observed (epoxy systems with 4 and 8 wt % PVAc) since less energy was required for the crack propagation. Such a difference in the failure mechanisms should be connected with the morphology of the samples.

Thermal Properties of the Blends

To check the thermal resistance of the systems DSC curves of the cured samples were considered and glass transition temperatures T_g were estimated (Figure 10). To ensure clearer determination of the glass transitions, 20 °C/min heating rate was chosen. It should be noted that in case of PVAc, as suggested earlier according to the samples appearance, phase separation takes place during curing and T_g of the second (PVAc-rich) phase is clearly seen at 8 wt % PVAc [Figure 10(a)]. At PVAc content lower than 4 wt %, this T_g is hardly seen and further decrease in the thermoplastic content does not allow any PVAc glass transitions to appear on the thermogram.

In case of PVB, the only glass transition observed at the curves is that of the epoxy resin. No indication of the PVB-rich phase T_g is seen even at the highest modifier content. So, DSC presumes absence of the phase transitions in epoxy–PVB matrices. Glass transition temperature values obtained by DSC are summarized in Table I. As seen from Table I, incorporation of thermoplastics generally leads to a drop in the glass transition temperature of epoxy-rich phase. The magnitude of the drop was almost the same for PVAc and PVB: a maximum decrease in the T_g of epoxy-rich phase was 7 °C for PVAc modifier, and

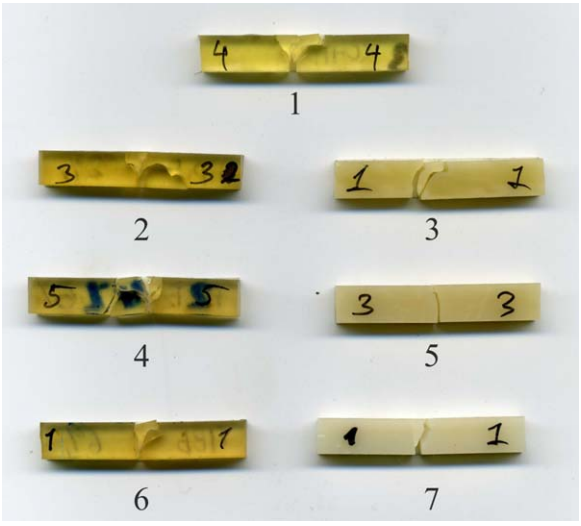

Figure 9. Pictures of the epoxy–thermoplastics samples after their failure under impact loading. Systems tested: (1) pristine unmodified epoxy resin, (2) epoxy–2 wt % PVB, (3) epoxy–2 wt % PVAc, (4) epoxy–4 wt % PVB, (5) epoxy–4 wt % PVAc, (6) epoxy–6 wt % PVB, and (7) epoxy–8 wt % PVAc. [Color figure can be viewed in the online issue, which is available at wileyonlinelibrary.com.]

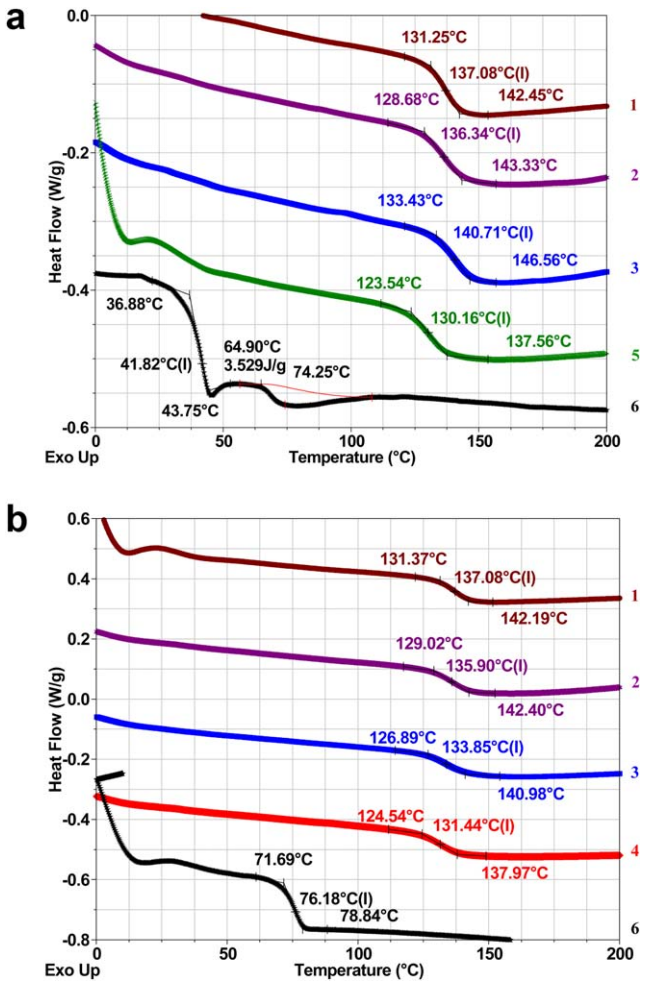

Figure 10. DSC thermograms of the cured epoxy–PVAc (a) and epoxy–PVB (b) systems. Thermoplastic content: (1) 0 wt %, (2) 2 wt %, (3) 4 wt %, (4) 6 wt %, (5) 8 wt %, and (6) 100 wt %. [Color figure can be viewed in the online issue, which is available at wileyonlinelibrary.com.]

5 °C for PVB modifier. It can still be regarded as quite moderate—due to the low modifier content.

T_g was also estimated by means of the torsion pendulum as a temperature point connected with abrupt drop of the storage modulus at increasing temperature. The results obtained are presented in Figure 11 and Table I. The same as in DSC, T_g of the second (epoxy-rich) phase decreased with modifier content. The behavior of shear modulus is even more remarkable. Incorporation of 2 wt % PVAc leads only to a light decrease in the shear modulus, without any changes of the pattern of its temperature dependence—due to the very low modifier content. However, addition of 4 and 8 wt % PVAc results in a significant decrease in the shear modulus already at 40 °C. It could be associated with glass transition of the PVAc-rich phase. A noticeable decrease of the loss tangent values is observed in the region of the glass transition of epoxy polymer, which is probably indicative of the fact that part of the epoxy polymer could be incorporated into the PVAc-rich phase. In case of 8 wt % PVAc shear modulus becomes too low already at the temperatures slightly higher than room temperature. It can be concluded that although incorporation of 4 wt % PVAc demonstrates G' values that are lower than those of pristine epoxy resin, the most notable decrease starts from 65 to 70 °C, which makes epoxy–4 wt % PVAc systems still acceptable for some applications from the practical point of view.

In case of PVB, almost no decrease in the G' values is observed after the thermoplastic incorporation. Moreover, for both 4 and 6 wt % PVB systems shear modulus values were slightly higher than those of pristine epoxy resin at temperatures below their T_g, which gives an additional advantage to PVB. However, the drop of the T_g values for epoxy–PVB systems is more noticeable than in case of PVAc modifier as obtained from the torsion pendulum, and a widening of the tan δ peak is observed due to PVB incorporation.

Table I. Glass Transition Temperatures of Epoxy–Thermoplastic Systems Determined by Various Methods

Thermoplastic content (wt %)	Glass transition temperature of the thermoplastic-rich phase $T_{g,1}$ (°C)			Glass transition temperature of the epoxy-rich phase $T_{g,2}$ (°C)		
	DSC	Tors. pend.	DMA	DSC	Tors. pend.	DMA
0	—	—	—	137	141	130
Epoxy–PVAc systems						
2	—	—	—	136	134	131
4	—	44	50	141	140	135
8	42	44	50	130	132	122
100	42	—	—	—	—	—
Epoxy–PVB systems						
2	—		—	136		128
4	—	—	—	134	132	122
6	—	—	—	131	130	129
100	73	—	—	—	—	—

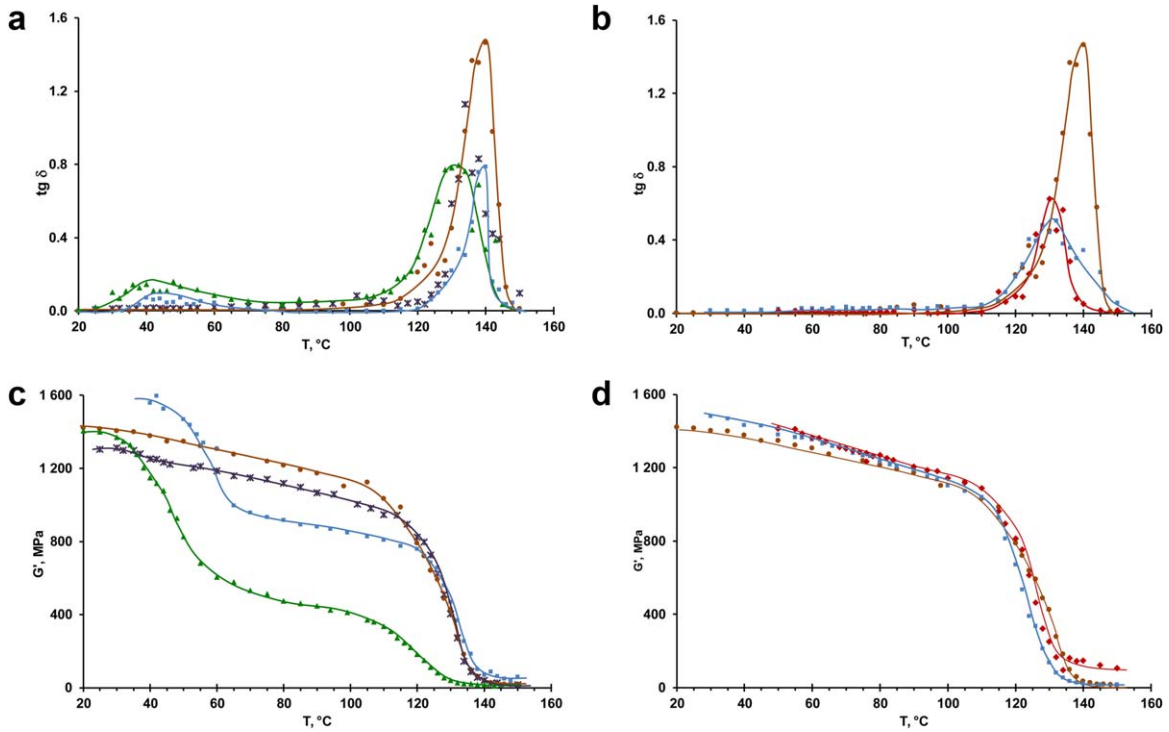

Figure 11. Loss tangent (a, b) and shear storage modulus (c, d) of epoxy–thermoplastic systems obtained at the torsion pendulum. Thermoplastic: (a, c) PVAc, (b, d) PVB. Modifier content, wt %: (0) ●, (2) ✱, (4) ■, (6) ◆, and (8) ▲. [Color figure can be viewed in the online issue, which is available at wileyonlinelibrary.com.]

The temperature dependence of elastic modulus E' measured by DMA technique is shown in Figure 12. It can be seen that the elastic modulus deteriorates significantly in the temperature range 40–50 °C in case of 4 wt % of PVAc Such a decrease is even more prominent for the system with 8 wt % PVAc. As for PVB, its introduction did not result in any notable E' changes—due to, possibly, absence or low content of PVB-rich phase and low modifier content.

The changes in the glass transition temperatures of the systems determined by DMA technique agree with the trends obtained by DSC and torsion pendulum methods, namely: appearance of only one glass transition temperature for PVB systems and two temperatures—for PVAc modifier, and an overall trend to a T_g decrease with modifier content growth.

An interesting fact worth noticing is abnormally high $T_{g,2}$ of epoxy-rich phase of the system with 4 wt % of PVAc, deviating from the general trend towards $T_{g,2}$ decrease (Table I). This fact was confirmed by all the methods used. Further modifier incorporation led to a decrease in the $T_{g,2}$ as it was expected. This phenomenon could be explained by the following considerations. It is a well-known fact,[9] that modifiers influence on the glass transition temperature of the matrix is highly dependent on the processes taking place during phase separation. Usually, phase separation is not complete, and both phases contain a small amount of the second component. Since glass transition temperatures of PVAc and PVB are lower than that of the cured epoxy polymer, their presence in the epoxy-rich phase should leads to a decrease in its T_g. At the same time, it was shown[34] that presence of a small amount of thermoplastic in the process of the phase separation could lead to a decrease in the viscosity of the system during curing. As a result, mobility of the epoxy phase increases and the final conversion of the epoxy matrix could rise, leading to an increase in the epoxy phase T_g. However, further thermoplastic content increase contributes to the viscosity buildup, decreases the mobility of the reactive system. Consequently, the conversion and T_g of the system deteriorate. So, T_g of the epoxy-rich phase could either deteriorate with an increase in the thermoplastic content, or have a maximum. In our case such a maximum is observed for epoxy–PVAc systems, whereas PVB incorporation causes just a monotonous decrease in the epoxy-phase T_g.

Morphology of Epoxy–Thermoplastic Systems

Typical micrographs illustrating the structure and morphology of the epoxy–PVAc cured systems are demonstrated in Figure 13. Epoxy–2 wt % PVAc system is characterized by the matrix-inclusion structure [Figure 13(a)], when the typical size of the dispersed phase is 1–2 μm. Such structure is also referred to as "sea-island" morphology in the literature.[35] The matrix is composed mostly of the epoxy polymer, with the dispersed phase enriched with PVAc.

An increase in the PVAc content up to 4 wt % [Figure 13(b)] drastically changes the morphology formed during the curing. It's obvious from the photo with low magnification that the system is macro inhomogeneous [Figure 13(b)] and, in spite of the low thermoplastic content, phase inversion is already starting. XRD microanalysis confirmed that the dark areas

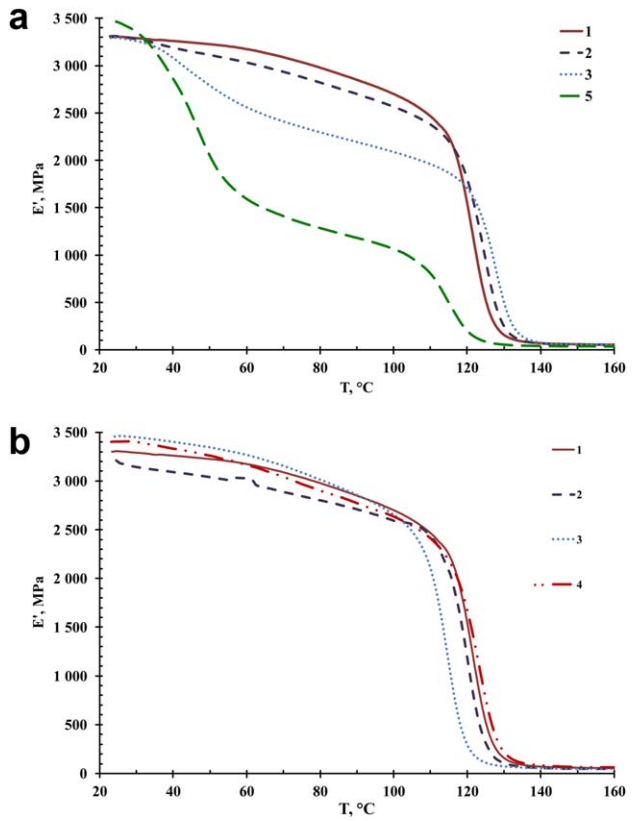

Figure 12. Elastic storage modulus of epoxy–thermoplastic systems obtained by DMA technique. Thermoplastic modifier: (a) PVAc, (b) PVB. Modifier content: (1) 0 wt %, (2) 2 wt %, (3) 4 wt %, (4) 6 wt %, and (5) 8 wt %. [Color figure can be viewed in the online issue, which is available at wileyonlinelibrary.com.]

correspond to an epoxy-rich phase, while light domains indicate a PVAc-rich one. High magnification images [Figure 13(c)] show that the morphology of the epoxy-rich domains is similar to that of the 2 wt % PVAc system. At the same time PVAc-rich domains [Figure 13(d)] contain dispersed phase of 5–10 μm size. The local element microanalysis revealed that this dispersed phase consists mostly of epoxy polymer.

Such a complex multilevel structure of a cured system is usually referred to as phase-in-phase morphology or double-phase morphology.[21] Primary morphology of epoxy-rich and PVAc-rich domains was generated at the beginning of the cross-linking reaction. In this case, the system viscosity is still low, translational mobility of components is high and, as a result, a high rate of the phase separation is observed. Later on, when the viscosity of the epoxy-rich phase is too high, phase separation can only continue locally. So, in the epoxy-rich macrophase PVAc-rich particles are still phase separated from the thermosetting polymer as conversion increases, but they cannot coalesce with the continuous PVAc-rich macrophase. In the PVAc-rich macrophase oversaturation quickly grows, which results in the secondary phase separation. A low translational mobility of macromolecules entrapped within the chemical epoxy network suppresses the particles growth. As a result, dispersed epoxy-rich spherical domains (up to 10 μm) are formed in the PVAc-rich macrophase.

Further PVAc content increase up to 8 wt % [Figure 13(e)] leads to a complete phase inversion in the system. In this case, also a "matrix-inclusions" structure is formed with the 1–3 μm epoxy-rich dispersed phase.

It should be noted that similar range of morphologies was described earlier for the numerous epoxy–thermoplastic systems, including the processes of the secondary phase separation.[5,6,9,21] Moreover, the content of the thermoplastic, corresponding to the phase inversion processes, is quite agreeable in our case with the results of other researchers. For example, such a phase inversion was shown to be completed already for 10 wt % polysulfone in epoxy resin cured by the anhydride hardener.[21]

The structure changes in the investigated systems can be elucidated with the help of the epoxy oligomer—PVAc phase diagram, obtained earlier (Figure 14).[36] The formation of the three-dimensional network of the chemical bonds during the process of curing results in a dramatic viscosity increase in the system. So, translational mobility of the components decreases and they are becoming more thermodynamically immiscible. Two-phase region of the phase diagram (Figure 14, region II) expands both along temperature and concentration axes. The concentration related to the upper critical solution temperature (UCST) point of the phase diagram is shifted into the region of the high thermoplastic contents, according to the classical Flory–Huggins–Scott theory of the polymer solutions[37]

$$\varphi_{cr2} = \frac{\sqrt{r_1}}{\sqrt{r_1}+\sqrt{r_2}} \quad (7)$$

where r is the component's degree of polymerization, and φ_{cr}—critical concentration.

So, at the start of curing at 90 °C A, B, and D points, corresponding to the systems investigated (2, 4, and 8 wt % PVAc), are located above the bimodal curve. As curing proceeds, the binodal shifts in the upper direction, so that the points A, B, and D are below the bimodal, in the two-phase area. Furthermore, they appear in the different parts of the two-phase area of the phase state diagram [Figure 15(a)]: in the regions enriched with PVAc (IIa), with epoxy oligomers (IIc), and region of the phase inversion (IIb). Since phase separation is initiated already at the conversion less than 0.08, the phases are formed at the high values of the diffusion coefficients, which provides their large sizes.

Micrographs of the cured epoxy–PVB systems are demonstrated in Figure 16. As can be seen from Figure 16(a), SEM did not allow us to see the phase structure of our systems clearly and so, TEM was tried [Figure 16(b–d)]. It was found out that independent of the PVB content, a matrix-inclusion morphology was formed, with the 50–100 nm size of the dispersed phase for all PVB contents. Such a small and uniform phase size independent of the PVB content seems to indicate that phase separation started in the gelation region, when epoxy conversion is high and translational components mobility is low. So, notable PVB-rich particles growth was impossible because of the diffusional restrictions. As a result, globular structure of the matrix enriched with epoxy polymer can be seen for all the systems [Figure 16(b,c)], with PVB prevalence in the dispersed particles.

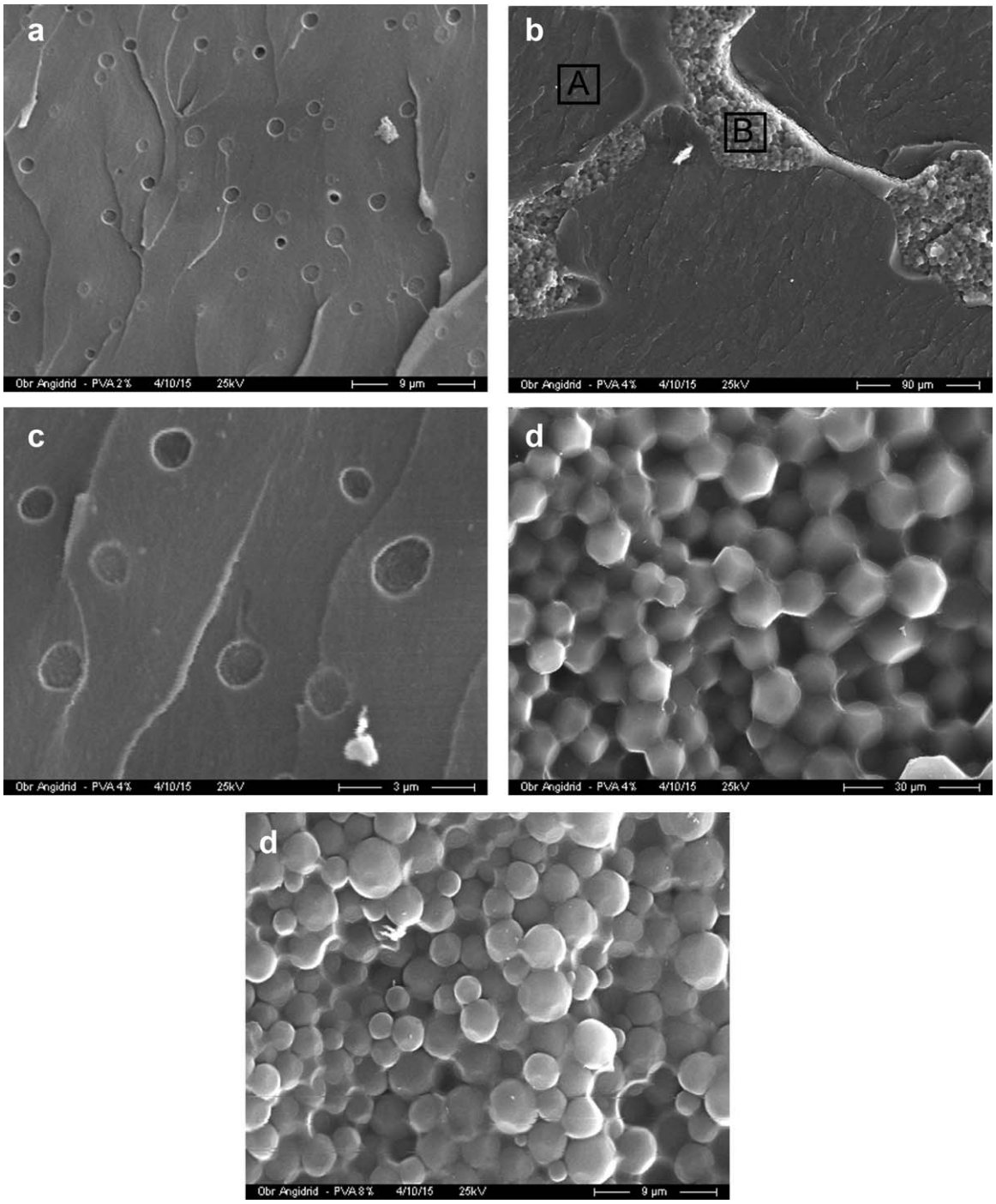

Figure 13. SEM micrographs of the cured epoxy–PVAc systems. PVAc content: (a) 2 wt %, (b) 4 wt %, (e) 8 wt %. (c) and (d) - higher magnification of the continuous phases: (c) fragment A, (d) fragment B.

These observations could be explained by assuming the big difference between the position of UCST on the phase diagram for the initial uncured system and the curing temperature [Figure 14(b)]. In this case, the bimodal curve shifts in the course of curing in such a way that the points A, B, and C, corresponding to all the epoxy–PVB systems studied (2, 4, and 6 wt % PVB), initially located in the single-phase area above the bimodal, turn out at the II_a region, that is, in the region of the formation of dispersed phase enriched by PVB. Widening of the II_a region in comparison with the phase diagrams for PVAc is connected with the obvious shifting of the critical temperature in the direction of the lower molecular weight PVB, according to Flory–Huggins–Scott theory.[37]

DISCUSSION

Studies of the morphology and phase structure of the epoxy–PVB and epoxy−PVAc systems allowed us to explain the

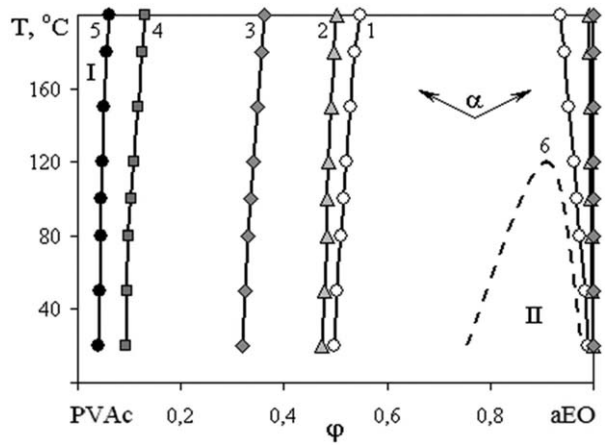

Figure 14. Phase diagrams of the PVAc—partly cured epoxy oligomers (aEO) systems. Conversion α: (1) 0.08, (2) 0.09, (3) 0.14, (4) 0.22, (5) 0.29, and (6) 0.07÷0.08. Hardener: diethylenetriamine. Dashed line shows the calculated phase diagram. I—single-phase (i.e., true solution) region, II—two-phase state region. The directions of the phase diagram evolution with the conversion increase are shown by the arrows. Data from Ref. 36.

patterns obtained in case of the mechanical properties. To summarize the data on the processes taking place in the systems, the following main features could be mentioned:

- Possible chemical interaction of the PVB with the epoxy resin/anhydride hardener system and possibility of PVB involvement into the epoxy resin network;
- Macrophase separation in epoxy−PVAc systems, with the phase inversion starting already at 4 wt %. The size of the dispersed (PVAc) phase could be up to 5–10 μm.
- Microphase separation in the epoxy/PVB systems, no phase inversion takes place. The size of the dispersed phase is 50–100 nm.

As demonstrated in "Mechanical Properties of the Blends" section, an increase in G_{IR} of the PVAc/epoxy matrices, starting already at 2 wt % modifier was obtained (Figure 6). At 2 wt % PVAc an enhancement of the fracture toughness should be connected with the "matrix-inclusions" structure of the cured system having the dispersed phase particles of 1–2 μm. So, as it was stated in ref. 38 for the epoxy–polysulfone systems with similar morphology, the following mechanisms seem to be dominant in this case: dissipation of the energy of the crack growth together with the crack path deflection and crack pinning. Further fracture toughness enhancement in case of the systems containing 4 and more wt % PVAc is stipulated by the formation of the structures with co-continuous morphologies. In this case, the front of the propagating crack is always in contact with the thermoplastic-rich phase that can dissipate the energy of the crack growth most effectively through the plastic deformation.[39]

An increase in the PVAc content up to 8 wt % does not lead to any further growth of the G_{IR} of the system—phase inversion has finished, and the matrix is a PVAc-riched phase with small epoxy resin domains. So, as before, the front of the crack is propagating through the more plastic PVAc matrix. Similar behavior—a notable increase in the fracture toughness, for the phase-separated matrices with continuous thermoplastic phases was described for epoxy resins in Refs. 5, 6, 9, and 21 and for dicyanate matrix modified with PEI.[13]

Influence of the PVB on the pristine epoxy resin fracture toughness is not as notable due to the very small size of the dispersed PVB phase—less than 100 nm. So, there could be two reasons for the slight increase in the PVB/epoxy system fracture toughness:

- crack path deflection and dissipation of the energy of the crack growth—the same mechanisms as acting in epoxy–2 wt % PVAc systems;
- possibility of the PVB involvement in the chemical cross-linking reaction. Epoxy resin network would become slightly less dense and not so rigid in this case.

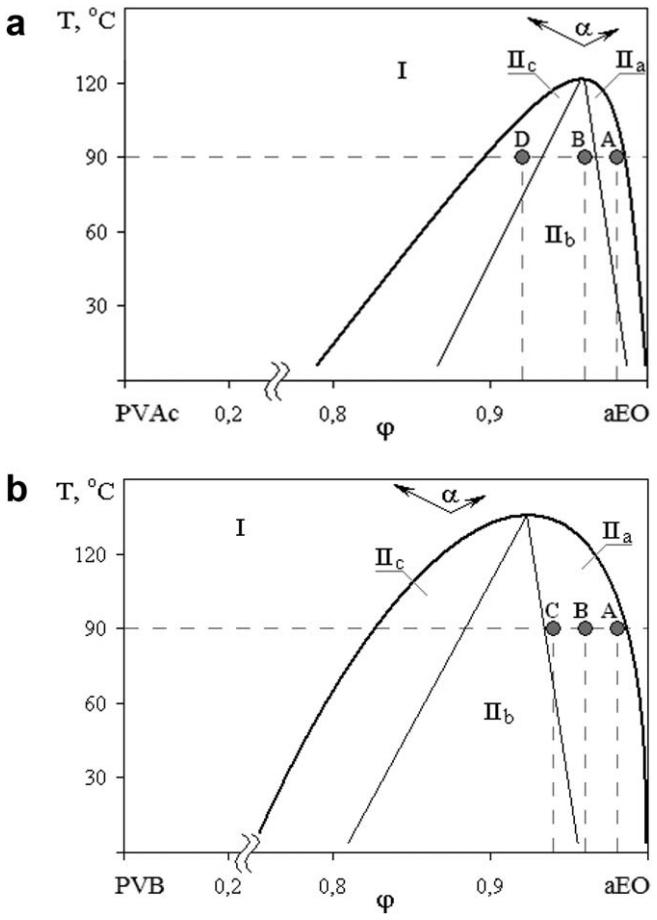

Figure 15. Scheme showing the position of the hypothetic epoxy–thermoplastic phase diagram binodal and the systems under investigation in the curing process. Thermoplastics: (a) PVAc, (b) PVB. A, B, C, D points correspond to 2, 4, 6, and 8 wt % thermoplastic in epoxy matrix respectively, 90 °C curing. I—region of the true solution, II—two-phase region. II_a, II_c—regions of the disperse phases enriched with PVAc and epoxy oligomers, respectively. II_b—region of the phase inversion. The directions of the phase diagram evolution with the conversion increase are shown by the arrows.

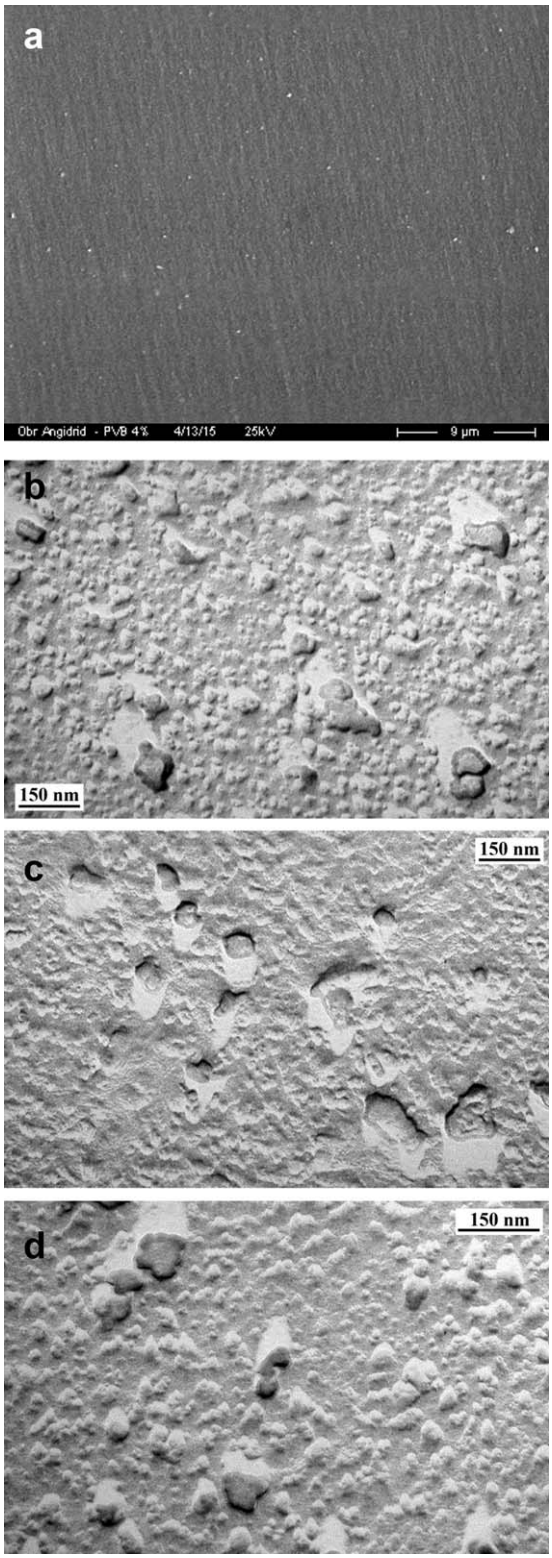

Figure 16. SEM (a) and TEM micrographs of the cured epoxy—PVB system. PVB content: (b) 2 wt %, (a), (c) 4 wt %, and (d) 6 wt %.

Similar situations were described in the literature, when only a small fracture toughness increase was observed for the systems with such a structure.[9,35] The reasons for a further decrease in the G_{IR} of our systems with the PVB incorporation are not clear, they require further investigations.

Impact loading results differ: an increase in the impact characteristics was observed only for the systems that have small thermoplastic-rich domains distributed in the continuous epoxy-rich phase. It could be supposed that when a crack propagates with the high rate, the energy is not dissipated by crack passing around the microphases. On the contrary, the crack front can go through the microphase and destroy it. It would still require extra energy, so, some increase in the impact characteristics could still be evidenced, although not too high. In case of co-continuous structures or phase inversion when the PVAc-rich phase becomes continuous, its lower strength leads to a decrease in the impact strength.

CONCLUSIONS

The potential of PVAc and PVB application for epoxy resin toughening was investigated, along with the thermal and mechanical properties of the resulting blends and their morphology. The following results were obtained:

- Both modifiers are soluble in epoxy oligomer/anhydride hardener systems, with the phase separation taking place during curing.
- Epoxy–PVB systems have matrix-inclusion morphology up to the highest content used (6 wt %): PVB-rich phase (50–100 nm size) dispersed in the epoxy-rich phase. Such a small size of the phase together with the low modifier content is considered as the reason for the inability of the conventional T_g measurement techniques to reveal the presence of this phase.
- Epoxy–2 wt % PVAc matrices are characterized by the sea-island morphology with the PVAc-rich phase dispersed in the epoxy-rich phase. At 4 wt % PVAc the phase inversion starts, when co-continuous morphologies are formed. At 8 wt % PVAc forms a continuous phase, with the epoxy-rich domains distributed in it.
- T_g of the epoxy-rich phase gradually decreases with an increase in thermoplastic content according to DSC, DMA, and torsion pendulum measurements. An overall decrease in the T_g could be up to 6–11 °C for the highest modifier concentration used (8% for PVAc and 6% for PVB). A notable drop in shear and elastic moduli of epoxy–PVAc systems is observed already at 40–50 °C—due to transition of PVAc-rich phase to the rubbery state. Small size of the PVB-rich phase restricts its influence on the shear and elastic moduli of the epoxy resin.
- Incorporation of the PVAc modifier resulted in an up to 2.4-fold increase in fracture toughness of pristine epoxy resin due to the following mechanisms: plastic deformation of the PVAc-rich phase, together with the crack path deflection and crack pinning. Maximum increase in the fracture toughness for epoxy–PVB systems was 45%, demonstrated by the 4 wt % PVB.
- Morphologies without a continuous thermoplastic-rich phase were shown to be the most effective for high impact properties. As a result, epoxy–PVB systems demonstrated 50–80%

enhancement in the impact strength and failure energy. PVAc usage (4 and 8 wt %) led to the deterioration of the impact epoxy resin properties—up to 30–60%.

REFERENCES

1. Epoxy Resin Chemistry and Technology; May, C. A., Tanaka, G. Y., Eds.; Marcel Dekker: New York, **1973**.
2. Kinloch, A. J.; Shaw, S. J.; Tod, D. A.; Hunston, D. L. *Polymer* **1983**, *24*, 1341.
3. Daly, J.; Pethrick, R. A.; Fuller, P.; Cunliffe, A. V.; Datta, P. K. *Polymer* **1981**, *22*, 32.
4. Solodilov, V. I.; Gorbatkina, Y. A.; Kuperman, A. M. *Mech. Comp. Mater.* **2003**, *39*, 493.
5. Martinez, I.; Martin, M. D.; Eceiza, A.; Oyanguren, P.; Mondragon, I. *Polymer* **2000**, *41*, 1027.
6. Min, B. G.; Hodgkin, J. H.; Stachurski, Z. H. *J. Appl. Polym. Sci.* **1993**, *50*, 1065.
7. Antonov, A. V.; Zelenskiy, E. S.; Kuperman, A. M. *J. Reinf. Plast. Compos.* **2003**, *22*, 361.
8. Teng, K. C.; Chang, F. C. *Polymer* **1996**, *37*, 2385.
9. Mimura, K.; Ito, H.; Fujioka, H. *Polymer* **2000**, *41*, 4451.
10. Bucknall, C. B.; Partridge, I. K. *Polymer* **1983**, *24*, 639.
11. Kalaev, D. V.; Brantseva, T. V.; Gorbatkina, Y. A.; Kerber, M. L.; Kravchenko, T. P.; Salazkin, S. N.; Shaposhnikova, V. V. *Polym. Sci. Ser. A* **2003**, *45*, 465.
12. Korokhin, R. A.; Solodilov, V. I.; Gorbatkina, Y. A.; Shapagin, A. V. *Mech. Compos. Mater.* **2015**, *51*, 313.
13. Hourston, D. J.; Lane, J. M. *Polymer* **1992**, *33*, 1379.
14. Gorbunova, I. Yu.; Kerber, M. L.; Shustov, M. V. *Plastmassi* **2003**, *12*, 38. In Russian.
15. Brooker, R. D.; Kinloch, A. J.; Taylor, A. C. *J. Adh.* **2010**, *86*, 726.
16. Zheng, S.; Hu, Y.; Guo, Q.; Wei, J. *Colloid. Polym. Sci.* **1996**, *274*, 410.
17. Prolongo, M. G.; Arribas, C.; Salom, C.; Masegosa, R. M. *J. Appl. Polym. Sci.* **2007**, *103*, 1507.
18. Sanchez-Cabezudo, M.; Masegosa, R. M.; Salom, C.; Prolongo, M. G. *J. Therm. Anal. Calorim.* **2010**, *102*, 1025.
19. Salimi, A.; Omidian, H.; Zohuriaan-Mehr, M. J. *J. Adh. Sci. Technol.* **2003**, *17*, 1847.
20. Badr, M. M.; Mansour, N. A.; Abulyazied, D. E.; Amer, M. S.; Moustafa, H. Y.; Ali, I. M.; Motawie, A. M. *Aust. J. Basic Appl. Sci.* **2012**, *6*, 666.
21. Oyanguren, P. A.; Galante, M. J.; Andromaque, K.; Frontini, P. M.; Williams, R. J. J. *Polymer* **1999**, *40*, 5249.
22. Jain, R.; Kukreja, P.; Narula, A. K.; Chaudhary, V. *J. Appl. Polym. Sci.* **2006**, *100*, 3919.
23. Xu, J.; Holst, M.; Rüllmann, M.; Wenzel, M.; Alig, I. *J. Macromol. Sci. Part B: Phys.* **2007**, *46*, 155.
24. Petrova, A. P. Klejaschie Materiali. Spravochnik (Glue Materials. Handbook). Redaktsija zhurnala "Kauchuk i rezina": Moscow, **2002**. In Russian.
25. Chalikh, A. E.; Gerasimov, V. K.; Mikhailov, Yu. M. Diagrammi Phasovogo Sostojanija Polimernikh System (Phase State Diagrams of Polymer Systems). Janus-K: Moscow, **1998**. In Russian.
26. Canè, F.; Capaccioli, T. *Eur. Polym. J.* **1978**, *14*, 185.
27. Polymer Data Handbook; Mark, J. E., Ed.; Oxford University Press: New York, NY, **1999**.
28. Praktikum po Polimernomu Materialovedeniju (Tutorial in Polymer Materials Science); Babaevskii, P. G., Simonov-Emeljanov, I. D., Eds.; Khimija: Moscow, **1980**. In Russian.
29. Petrova, I. I. Issledovanije Protsessa Vzaimodejstvija Polimerov s Plazmoj Visokotchastotnogo Kislorodnogo Razrjada (Investigation of the Interaction between Polymers and High Frequency Oxygen Plasma). D.Sc. dissertation, Institute of Physical Chemistry AS USSR, **1973**.
30. Chalikh, A. E.; Aliev, A. D.; Rubtsov, A. E. Elektronno-Zondivij Mikroanaliz v Issledovanii Polimerov (Electron Probe Microanalysis in Polymer Research); Nauka: Moscow, **1990**. In Russian.
31. Schimmel, G. Elektronenmikroscopische Methodik; Springer-Verlag: Berlin/Heidelberg/New-York, **1969**.
32. Sultan, S. R.; Salah, N. J.; Abdul Razak, A. A. *Al-Taqania* **2010**, *23*, 35.
33. Solodilov, V. I.; Korokhin, R. A.; Gorbatkina, Yu. A.; Kuperman, A. M. *Mech. Compos. Mater* **2015**, *51*, 177.
34. Kazakov, S. I.; Kerber, M. L.; Gorbunova, I. Y. *Polym. Sci. Ser. A* **2005**, *47*, 1001.
35. Min, H. S.; Kim, S. C. *Polym. Bullet.* **1999**, *42*, 221.
36. Shapagin, A. V. Structuroobrazovanije v Sistemakh Epoksidnije Oligomeri—Termoplasti (Structure Formation in Epoxy Oligomers-Thermoplastics Systems). Ph.D. Thesis, Institute of Physical Chemistry RAS, November **2004**.
37. Malkin, A. Ya.; Chalikh, A. E. Diffuzija i Vjazkost' Polimerov. Metodi Izmerenija (Polymers Diffusion and Viscosity. Measurement Techniques); Khimia: Moscow, **1979**.
38. Huang, P.; Zheng, S.; Huang, J.; Guo, Q.; Zhu, W. *Polymer* **1997**, *38*, 5565.